PNAS

Supporting Information for

Insight into the mechanism of H^+-coupled nucleobase transport.

Jun Weng[†], Xiaoming Zhou[†], Pattama Wiriyasermkul[†], Zhenning Ren, Kehan Chen, Eva Gil-Iturbe, Ming Zhou[*] Matthias Quick[*]

[†] Jun Weng, Xiaoming Zhou and Pattama Wiriyasermkul contributed equally.

*Corresponding Authors: Matthias Quick and Ming Zhou.

Email: mq2102@cumc.columbia.edu and mzhou@bcm.edu.

This PDF file includes:

Supplementary Figures 1 to 7
Supplementary Table 1
Supplementary References

Supplementary Figures and Tables

Supplementary Figure 1

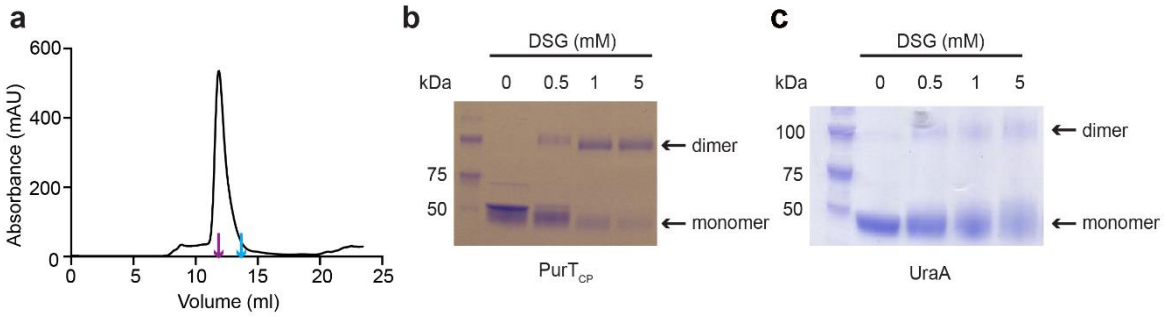

Supplementary Figure 1. Purification and crosslinking of $PurT_{Cp}$. a. Size-exclusion chromatography of $PurT_{Cp}$ in DDM. Elution volumes of membrane proteins of known molecular weight, bcMalT (100 kDa, purple) (1) and mouse SCD1 (41 kDa, blue) (2) are marked by arrows. **b-c**. SDS-PAGE showing Crosslinking of purified $PurT_{Cp}$ (**b**) or UraA (**c**) by disuccinimidyl glutarate (DSG).

Supplementary Figure 2

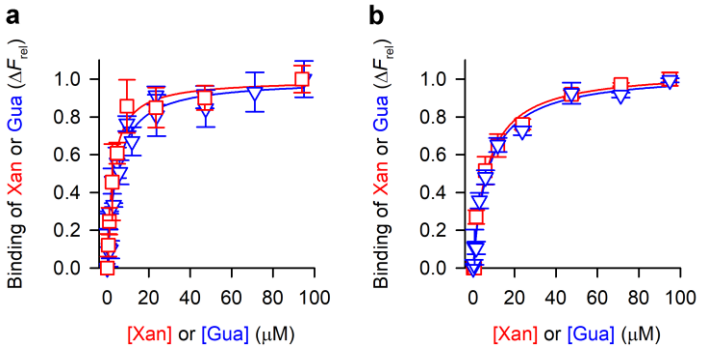

Supplementary Figure 2: Substrate binding kinetics of PurT$_{Cp}$. Saturation binding of xanthine (red) or guanine (blue) to 0.5 µM of purified PurT$_{Cp}$ was measured with microscale thermophoresis (MST) using **a.** the Monolith NT.LabelFree in conjunction with unlabeled PurT$_{Cp}$ or **b**. the Monolith NT.115 in combination with RED-tris-NTA-labeled PurT$_{Cp}$. Data of ≥ 6 independent experiments were subjected to non-linear regression fitting in Prism 8 and yielded a K_d for xanthine binding of 2.76 ± 0.4 µM and a K_d for guanine binding of 4.47 ± 0.75 µM with the label-free method (panel **a**). Fitting of data measured with the RED NT-647 dye-labeled PurT$_{Cp}$ yielded a K_d for xanthine binding of 6.81 ± 1.25 µM and a K_d for guanine binding of 7.37 ± 0.93 µM.

Supplementary Figure 3

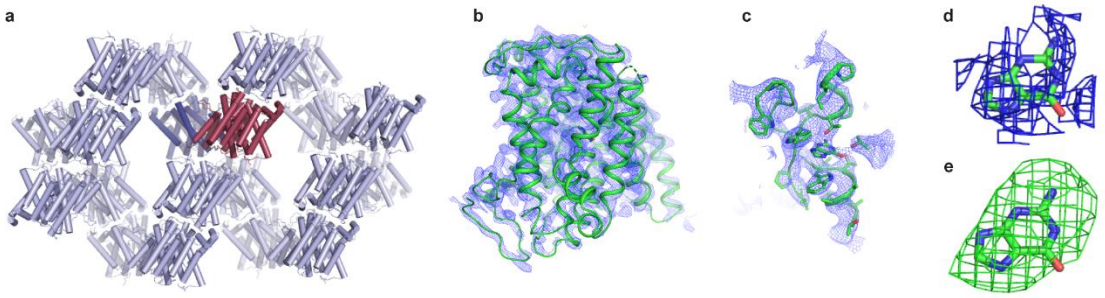

Supplementary Figure 3. Crystal packing and electron density of $PurT_{Cp}$. a. A cross-section of the crystal lattice in the UraA structure. One asymmetric unit is colored pink. **b.** $2F_O$-F_C map of a $PurT_{Cp}$ dimer contoured at 2 σ**. c**. $2F_O$-F_C map of a guanine molecule contoured at 1.0 σ. **d**. F_O-F_C map of a guanine molecule contoured at 2.5 σ.

Supplementary Figure 4

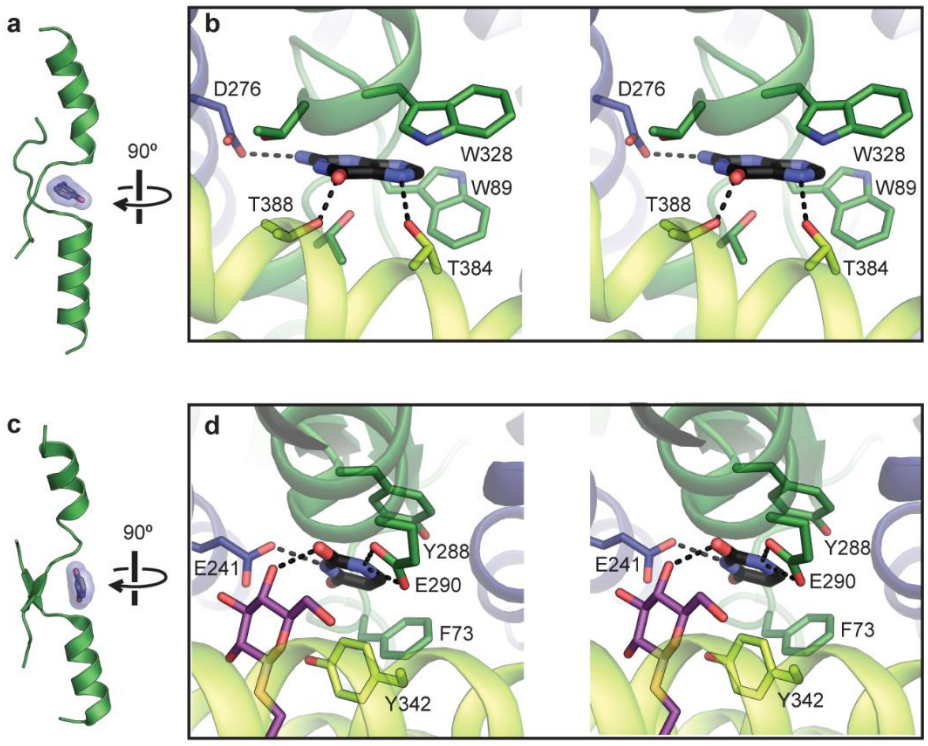

Supplementary Figure 4. Substrate binding site comparison between $PurT_{Cp}$ and UraA. a. The bound substrate (blue) in $PurT_{Cp}$ is shown in relation to the TM3 and TM10 transmembrane passes. **b.** Stereo view of the substrate-binding site in $PurT_{Cp}$, with nearby residues shown as sticks and potential hydrogen bonds marked with dashed lines. **c.** The bound substrate (blue) in UraA (PDB ID 3QE7) between TM3 and TM10. **d.** Stereo view of the substrate-binding site in UraA. A bound detergent molecule is shown as purple sticks.

Supplementary Figure 5

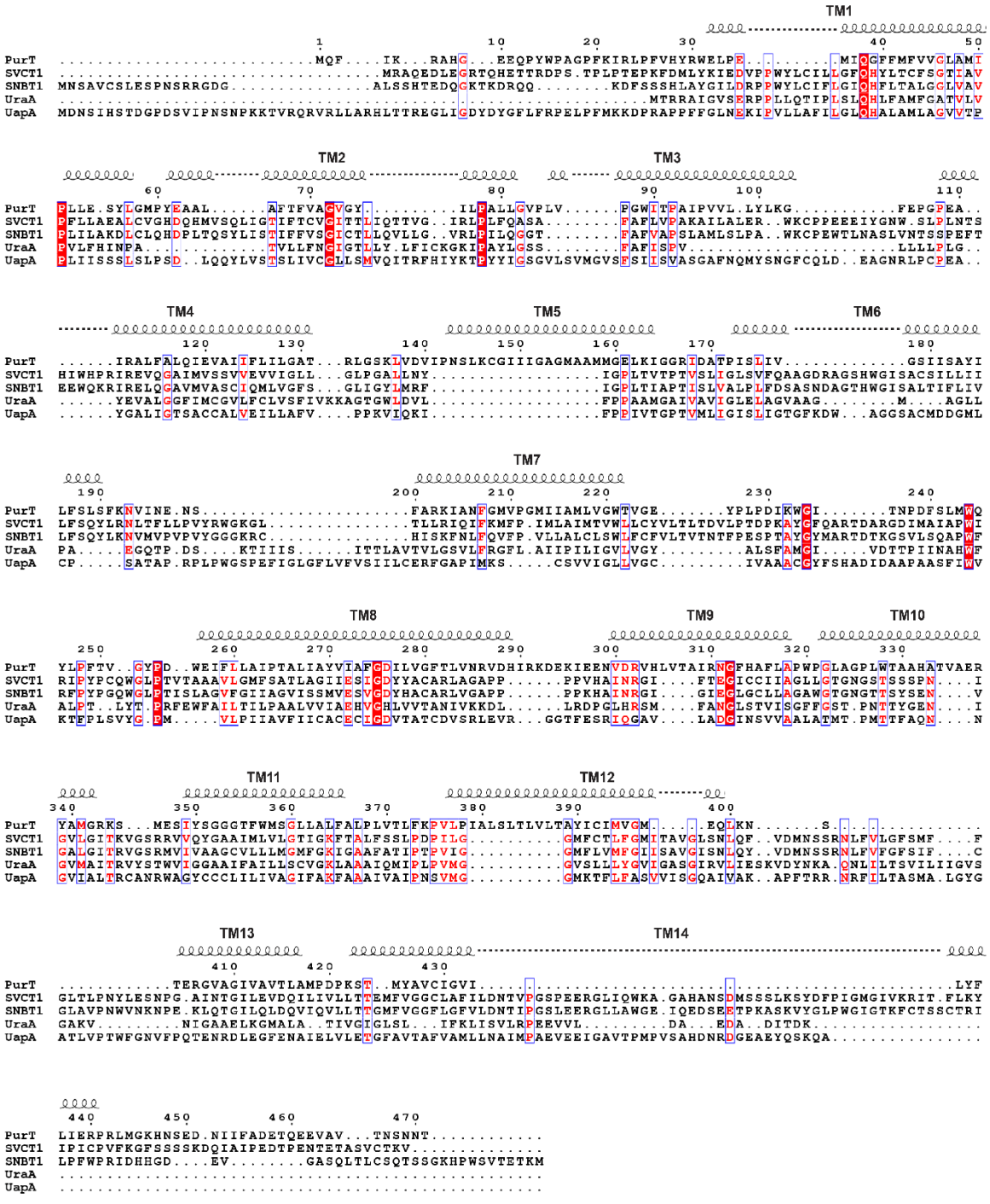

Supplementary Figure 5. Sequence alignment of PurT with selected NAT family members.

PurT (Gene Bank accession number OUR80909) from *Colwellia psychrerythraea* 34H; SVCT1

(Uniprot accession number BC050261), a human L-ascorbate transporter; SNBT1 (AB511909), an uracil transporter from rat; UraA (YP490725), an uracil transporter from *E. coli;* UapA (Q07307), a uric acid/xanthine H^+ symporter from *A. nidulans*. The selected sequences were aligned using Clustal Omega1 and plotted using Espript server. The secondary structure elements of PurT are indicated above the sequence. $PurT_{Cp}$ shares 12 % identity and 25.3 % similarity with human SVCT1 (SLC23A1), 12.9 % identity and 26.4 % similarity with rat SVCT1, 16.4 % identity and 31.4 % similarity with *E. coli* UraA, and 13.2 % identity and 25.6 % similarity with *A. nidulans* UapA.

Supplementary Figure 6

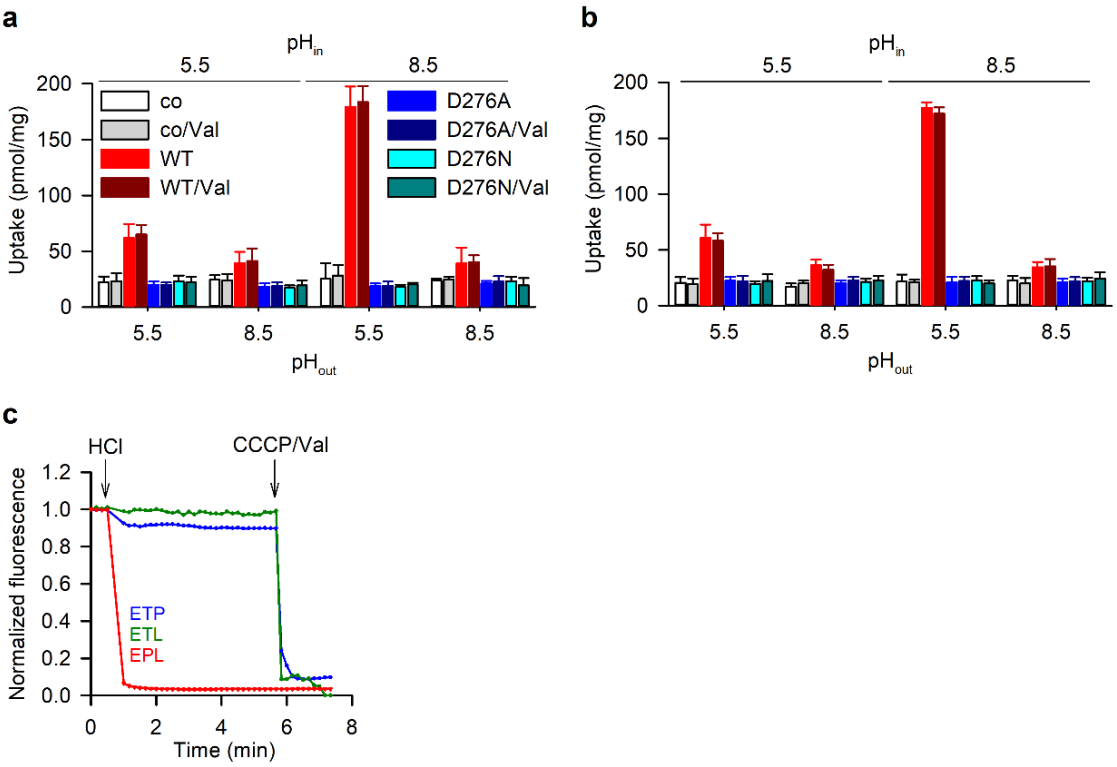

Supplementary Figure 6. Characterization of $PurT_{Cp}$-mediated transport. **a.** Effect of an inwardly-directed membrane potential. Uptake of 1 µM ^{3}H-xanthine by proteoliposomes containing $PurT_{Cp}$-WT, -D276A, or -D279N, or control liposomes prepared in 20 mM Hepes-KOH, pH 8.5, 100 mM KCl, 2 mM β-mercaptoethanol (pH_{in} = 8.5) or 20 mM Mes-KOH, pH 5.5, 100 mM KCl, 2 mM β-mercaptoethanol (pH_{in} = 5.5) was measured for 30 s in 20 mM Hepes-KOH, pH 8.5, 100 mM NaCl, 2 mM β-mercaptoethanol (pH_{out} = 8.5) or 20 mM Mes-KOH, pH 5.5, 100 mM NaCl, 2 mM β-mercaptoethanol (pH_{out} = 5.5) in the presence or absence of 1 µM of valinomycin (Val) as indicated. Under this condition, the addition of the potassium-selective ionophore valinomycin generated an outwardly-directed flux of K^+ that leads to the generation of an inwardly-directed electrical membrane potential (inside negative). **b.** Effect of an outwardly-directed membrane potential. Uptake of 1 µM ^{3}H-xanthine by proteoliposomes containing $PurT_{Cp}$-WT, -D276A, or -D279N or control liposomes (bar fills are identical to those shown in panel **a.**) prepared in 20 mM Hepes-KOH, pH 8.5, 100 mM NaCl, 2 mM β-mercaptoethanol (pH_{in} = 8.5) or 20 mM Mes-KOH, 100 mM NaCl, 2 mM β-mercaptoethanol (pH_{in} = 5.5) was measured for 30 s in 20 mM Hepes-KOH, pH 8.5 (pH_{out} = 8.5), 100 mM KCl, 2 mM β-mercaptoethanol or 20 mM Mes-KOH, pH 5.5, 100 mM KCl, 2 mM β-mercaptoethanol (pH_{out} = 5.5) in the presence or absence of 1 µM of valinomycin (Val) as

indicated. Here, the addition of valinomycin mediated the influx of K^+, leading to the generation of an outwardly-directed membrane potential (inside positive). Data are means ± S.E.M. of ≥ 3 independent experiments performed as technical triplicates. **c**) Test of H^+ leakage across liposome preparations(37). Liposomes made of *E. coli* polar lipids (EPL) or liposomes (ETL) and $PurT_{Cp}$-containing proteoliposomes (ETP) made of *E. coli* total lipids were loaded with 10 µM Oregon Green 514 carboxylic acid by freeze–thaw cycles and sonicated. After removing extraliposomal fluorophore by Sephadex G-50 column-based gel filtration, liposomes were diluted 10-fold, and the Oregon Green 514 fluorescence (excitation: 489 nm and emission: 524 nm) was monitored in a 96 well plate. The addition of HCl to yield an extraliposomal pH of ~2.4 led to a rapid decrease of fluorescence for EPL liposomes, indicating that H^+ can rapidly diffuse through the EPL membrane. In contrast, the extraliposomal acidification to pH of ~ 2.4 in ETL liposomes/proteoliposomes yielded only fractional internal acidification, suggesting that the pH gradient in this preparation is well maintained. As a positive control, the addition of the ionophores CCCP and valinomycin (1 µg/mL each) at the end of the experiment led to the collapse of the transmembrane pH gradient.

Supplementary Figure 7

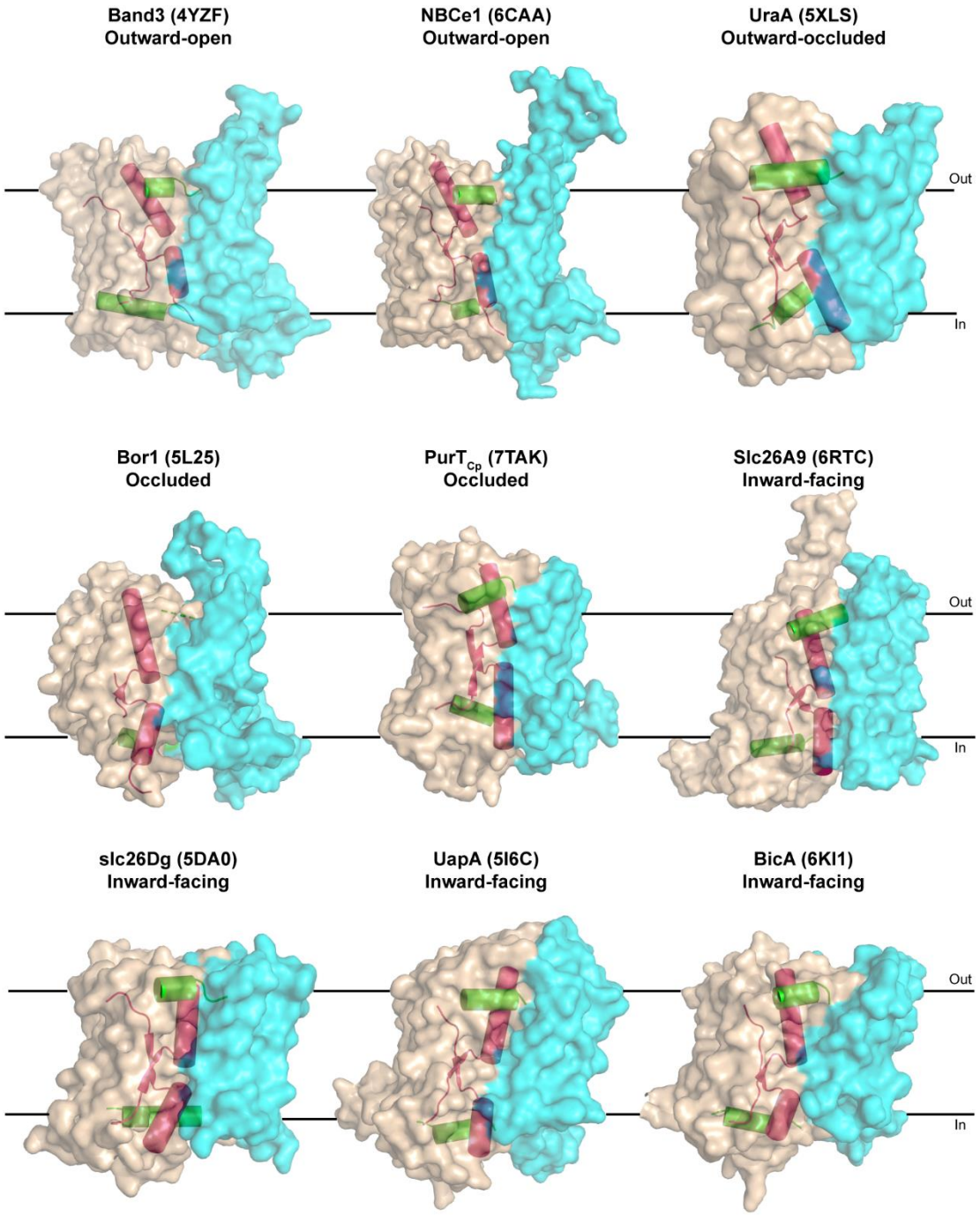

Supplementary Figure 7. Conformations of proteins with similar structural fold to PurT$_{Cp}$. One protomer of each protein is shown as cartoon representation. The scaffold domains are

colored cyan and the transport domains wheat. TM3 and TM10 that form the substrate binding site are highlighted as red cylinders. The two amphipathic helices that bridge the scaffold domain and the transport domain are shown as green cylinders.

Supplementary Table 1

Supplementary Table 1. Data collection and refinement statistics

Dataset	Native $PurT_{Cp}$
Data Collection	
Space group	P21212 (No. 18)
Unit cell (Å)	a=131.71, b=135.99 c=79.17
Wavelength (Å)	0.9150
Resolution (Å)	50.00 – 2.75 (2.80 – 2.75)
Completeness (%)	98.63 (90.43)
Redundancy	7.5 (6.1)
Mean I/σ	43.18 (2.17)
Refinement	
Resolution (Å)	41.78 – 2.80 (2.90 – 2.80)
Unique reflections	35,339 (3,186)
R_{work} (%) / R_{free} (%)	21.30/24.59
Number of non-hydrogen atoms	
Protein	6,847
Ligand/ion	22
Average B factors (Å^2)	
Protein	105.70
Ligand/ion	104.86
Rmsd	
Bond length (Å)	0.008
Bond angles (°)	1.19
Ramachandran plot (%)	
Favored	97.06
Allowed	2.94
Outliers	0.00
Rotamer outliers (%)	0.69

Statistics for the highest-resolution shell are shown in parentheses.

Supplementary References

1. Y. Bai *et al.*, X-ray structure of a mammalian stearoyl-CoA desaturase. *Nature* 524, 252-256 (2015).
2. Z. Ren *et al.*, Structure of an EIIC sugar transporter trapped in an inward-facing conformation. *Proc Natl Acad Sci U S A* 115, 5962-5967 (2018).